Disorder-Order Transitions in Soft Sphere Polymer Micelles

Glen A. McConnell,[1] Alice P. Gast,[1] John S. Huang,[2] and Steven D. Smith[3]
[1]*Department of Chemical Engineering, Stanford University, Stanford, California 94305*
[2]*Exxon Research and Engineering Company, Annandale, New Jersey 08801*
[3]*The Procter & Gamble Company, Cincinnati, Ohio 45239-8707*
(Received 23 June 1993)

Diblock copolymers in a selective solvent often assemble into spherical micelles. These micelles demonstrate long range order at moderate polymer concentrations. We explore the nature of the disorder-order transition in micellar suspensions through small angle x-ray diffraction studies. The phase behavior includes body-centered cubic (bcc) and face-centered cubic (fcc) lattices. We present the first phase diagram for block copolymer micelles to include both bcc and fcc structures and characterize the lattice selection by a ratio of coronal layer thickness to core radius.

PACS numbers: 83.70.Hq, 61.10.Lx, 64.60.Cn, 64.70.−p

Since the discovery of the Kirkwood-Alder transition in hard spheres [1], numerous disorder-order transitions have been elucidated in a variety of hard and soft sphere systems [2–5]. Experiments and computer simulations on charged colloidal suspensions indicate the formation of fcc ordered arrays when the Coulomb interaction, modeled as a Yukawa potential, is highly screened whereas bcc lattices are preferred when the screening is low [4,5]. While the experimental and simulation evidence for ordering in purely repulsive systems is mounting, understanding of the transition between bcc and fcc lattices is still limited. A convenient model for such a study is the suspension of spherical micelles formed by block copolymers dissolved in a solvent selective for one of the blocks. Such a system interacts via repulsions between the solvated chains forming the micellar corona and thus is amenable to alteration by changing the polymer composition. In this Letter, we describe the first phase diagram illustrating the influence of chain architecture on micellar ordering in solution. The chain architecture can be summarized in terms of the micellar dimensions and the resulting interactions are analogous to other soft sphere systems.

Diblock copolymers comprise chemically distinct polymers joined by a covalent bond. In this investigation we use a series of polystyrene-polyisoprene (PS-PI) diblock copolymers synthesized by anionic polymerization [6]; some of the polymers have perdeuterated polystyrene blocks (*d*-PS-PI). In Table I we list the diblock copolymers in terms of their molecular weights in thousands. The polydispersity index for these polymers is below 1.05; thus we treat them as monodisperse chains.

When diblock copolymers are placed in a solvent preferential for one block, they self-assemble to form spherical micelles above a critical polymer concentration (CMC). In this study of PS-PI diblock polymers, decane serves as a preferential solvent for polyisoprene. The micelles comprise a highly concentrated polystyrene core surrounded by a diffuse corona of polyisoprene. The micelles are in equilibrium with free (single) chains, but the CMC is so low (10^{-3}–10^{-2} wt.%) that the solution is dominated by micelles and single chain contributions to the scattering signal are negligible.

Micellization is an enthalpically driven process [7]. As

TABLE I. Dilute limit properties and phase behavior of PS-PI diblocks. All values reported in Å.

Polymer	Aggregation number	R_c $P(q)$	R_c solid	R_h	Lattice type	(Nearest neighbor)/2
d-PS-PI						
15K-15K	80	74	75	195	bcc	189
19K-8K	270	116	121	184		
20K-10K	235	117	119	220		
33K-22K	335	150	160	362	fcc	348
36K-36K	245	142	145	467		
44K-22K	420	204	186	484	fcc	454
40K-40K	90	106	108	296	bcc	259
45K-45K	130	137	127	450	bcc	378
h-PS-PI						
10K-20K		90[a]		210	fcc	204
31K-20K		148[a]		284		
46K-20K		204[a]		331	fcc	356

[a]Core radius determined from location of first minimum in x-ray form factor.

a result of the unfavorable enthalpic interactions between polystyrene and decane, the polymer suspension can reduce its free energy by forming spherical aggregates. The number of chains per micelle, or aggregation number, will vary with solvent quality and the molecular weight of the insoluble block [8]. We exploit this fact to generate a series of micelles of differing internal architecture. Diblocks having long polystyrene blocks and comparatively short polyisoprene blocks form micelles having large aggregation numbers with large cores and relatively thin coronas. Alternatively, by reversing the block ratios, we can produce micelles having lower aggregation numbers, small cores, and long coronal chains resembling a star polymer [9].

The micellar architecture serves as the most important experimental delineation within this series. Recent self-consistent mean field theories aptly demonstrate the influence of core curvature on the coronal density profile [10]. When the curvature is high as in the case of star polymers, the coronal density decays as $r^{-4/3}$ in a good solvent [11]. When the curvature is low, the density profile is described as chains tethered to a flat wall, known as a polymer brush. Chains attached to a planar interface in a good solvent at a surface concentration σ sufficient to cause them to stretch from their random coil configuration, $\sigma > N^{-6/5}$, assume a parabolic concentration profile [12]. In the limit of a very thin corona in comparison to the core size, the local curvature will be flat and well approximated by the parabolic profile. In contrast, coronal layers that are large compared to the core are well depicted by the starlike scaling model.

The coronal density profile is intimately related to the repulsive interactions between micelles [13]. Brushlike layers with their convex parabolic profiles provide steeper repulsions than interactions between polymer layers having starlike concave profiles. Although at this point no detailed model exists for the interactions between micelles, our experimental observations suggest that a description of the phase behavior in terms of the ratio of coronal layer to core size is adequate to qualitatively characterize the interaction.

In Table I we summarize the dilute solution properties of the polymers used in this investigation. We utilized *d*-PS-PI polymers to perform small angle neutron scattering (SANS) experiments at the National Institute of Standards and Technology. Deuterated and hydrogenated decane were mixed to match either the core (*d*-polystyrene) or coronal (polyisoprene) scattering densities. Scattering intensities from 0.5 wt.% diblock solutions in polyisoprene match solvents were fit to polydisperse solid sphere form factors, listed as R_c in Table I, using a Schulz distribution function. Additionally, the absolute intensity at zero angle provides the aggregation number through Zimm analysis. Using this aggregation number we calculate the radius of a space-filling core of polystyrene chains, denoted "R_c solid" in Table I. The results, shown in Table I, agree quite well when we compare the size of a solid core of polystyrene chains with the radius determined from the form factor fits. These studies suggest that the solvent swelling of the core is less than 10% by volume.

In principle, we would like to measure the coronal layer thickness, but this is not directly accessible. Measurements of the radius of gyration (R_g) either from SAXS or SANS (with polystyrene match solvent) offer only a measure of the contrast-weighted second moment of the coronal layer. Although we have obtained R_g in all cases, we cannot extract a polymer layer thickness without applying a model of the density profile. Instead, we choose to use a hydrodynamic layer thickness obtained from dynamic light scattering experiments (DLS). The hydrodynamic radius is defined as the radius that is assigned to the diffusion coefficient, D, obtained from DLS through the Stokes-Einstein expression, $R_h = kT/6\pi\mu D$. In practice the hydrodynamic radius is slightly smaller than the overall micelle radius, reflecting drainage in the outer regions of the micelle where the polymer concentration is very dilute. The hydrodynamic layer is a material property of the micelle depending primarily on the coronal density profile [14].

Interpretation of SAXS from micellar suspensions whose interactions are on a length scale commensurate with their physical dimensions poses some formidable challenges. The scattered intensity is a product of both intra- and intermicellar interference. In the case of x-ray scattering experiments, the intramicellar interference includes contributions from both the corona and the core. For PS-PI in decane the contrast is greatest for the core block generating form factors whose first minimum is denoted by the core-corona interface. In Figs. 1(a) and 2(a) we show intramicellar interference (form factors) for two such systems at dilute concentrations. Although the dilute limit properties are better studied by SANS where contrast matching techniques are utilized, the high resolution of x rays makes x-ray scattering preferable for diffraction studies.

Our high resolution x-ray diffraction studies performed at Stanford Synchrotron Radiation Laboratory, beamline 1-4 [15], serve as the basis for determining the phase behavior. When the crystallites are randomly oriented and much smaller than the beam size, the Bragg interference is a "powder" pattern including constructive interference from all **q** vectors spanning the reciprocal lattice.

The intensity profile is obtained by taking the product of the form factor with the crystal Bragg peaks. This leads to an intensity profile with sharp peaks weighted by both the Bragg degeneracy of each peak and the form factor. Real crystalline solids display a Gaussian distribution about their Bragg peaks attributed to the variability in lattice dimension and related to strain in the crystal. These modifications to the crystalline structure can make fits to the intensity profile subject to multiple parameters. Based on these limitations as well as the distinct possibility that the coronal layer is compressed at

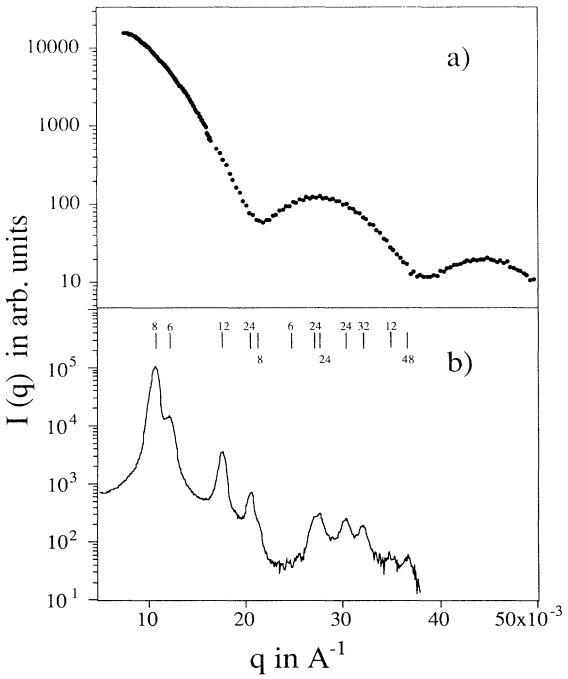

FIG. 1. (a) Form factor of *h*-PS-PI 46K-20K at 0.5 wt.% in decane. (b) Diffraction pattern from same micelles at 22%.

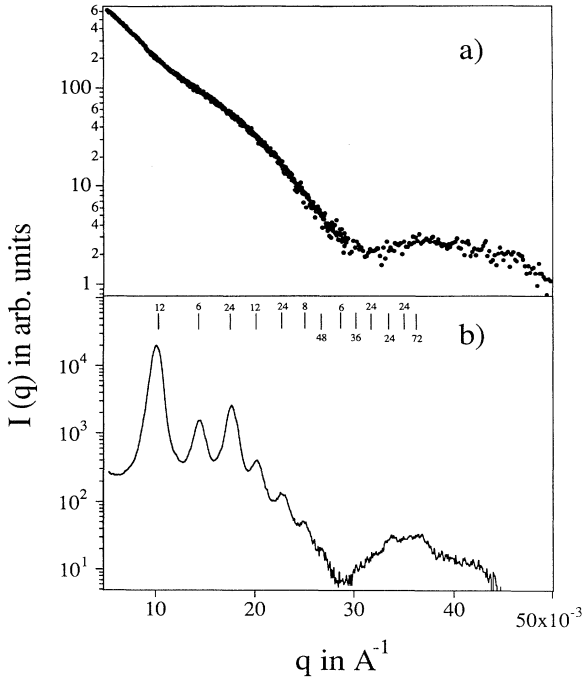

FIG. 2. (a) Form factor of *d*-PS-PI 45K-45K at 0.5 wt.% in decane. (b) Diffraction pattern from same micelles at 12.5%.

elevated concentrations, slightly altering the form factor, we choose to rely on the location of the Bragg peaks and a qualitative comparison of Bragg degeneracies in order to determine the lattice structure rather than model fits.

In addition, Nagler and co-workers [16] recently showed an intensity profile interpreted as the summation of a bcc solid and a disordered liquid, implying coexistence between the two phases. Certainly a study examining disorder-order transitions by increasing the polymer concentration will include the possibility of two-phase scattering. Even with these complications, the clear identification of several orders of Bragg peaks allows an unambiguous determination of the lattice structure and lattice constant based solely on the location of the Bragg peaks for an fcc crystal. In Fig. 1(b), the micelles observed in Fig. 1(a) have ordered into an fcc crystal at 22 wt.% polymer. The marks above the intensity profile indicate the locations of Bragg peaks with a lattice constant of 1007 Å. The numbers above and below the marks denote the true powder pattern degeneracy for the *n*th order Bragg peak of an fcc crystal. Similarly, we can compare the intermicellar interference for micelles formed from *d*-PS-PI 45K-45K; in this system, the micelles produce a bcc crystal at 12.5 wt.% as illustrated in Fig. 2(b). The marks denote a comparison with a bcc crystal having a lattice dimension of 872 Å. The faint presence of the seventh order Bragg peak is adequate to differentiate between bcc and simple cubic (sc). More convincingly, the intensity at the third order Bragg peak is larger than the intensity at the second order peak. Since the form factor is a decreasing function of q in this region, the degeneracy of the third order Bragg peak must be greater than that of the second order peak. The powder pattern of a bcc crystal does exhibit higher degeneracy in the third order Bragg peak while a sc does not. Based on this information we conclude that the micelles formed from *d*-PS-PI 45K-45K have ordered into a bcc crystal.

Several studies caused speculation about the possible crystal structure for particular diblock systems [17,18]. This speculation occurred for the most part because of the absence of higher order Bragg peaks which left the possibility of bcc or sc lattices. In this work the presence of higher order Bragg peaks allows conclusive determination of the crystal structure; this resolution allows us to demonstrate the first conclusive evidence for the existence of fcc crystals in diblock systems. Additionally, the minimum in the form factor denoting the interface between the core and the corona suggests that the micelles observed at dilute concentrations do not significantly change their structure upon increases to moderate polymer concentrations, and thus undergo disorder-order transitions at particular micelle concentrations exactly like particles with soft repulsive interactions. We show the variation of order-disorder and the preferred lattice behavior of diblock micelles as a function of concentration and architecture in Fig. 3.

The most remarkable aspect of this study is that variations in micellar structure give rise to disorder to order transitions that include both fcc and bcc crystals. A close analog of these micellar systems is the charged colloidal

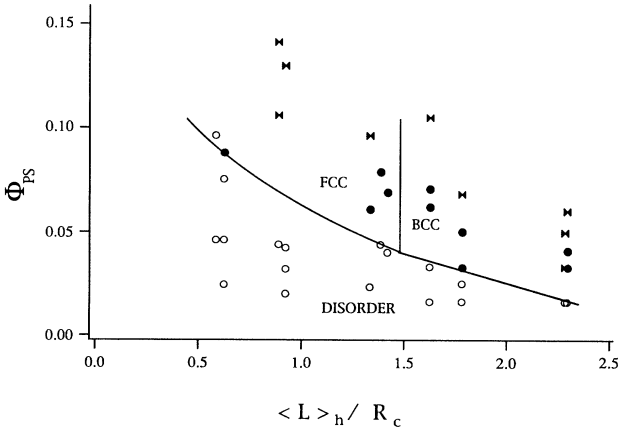

FIG. 3. Phase diagram depicting disorder (open circle) to order (closed circle) region and lattice type in terms of the polystyrene core volume fraction as a function of coronal layer thickness to core size. Unspecified structures are labeled (double triangle).

particle whose pair interaction is described by the Yukawa potential; the ionic strength of the solution defines the decay length. Experimental studies as well as Monte Carlo simulations demonstrate the relationship between the length scale of the interactions and the resulting stable, crystal structure [4,5]. As the repulsions become short ranged, the system favors an fcc solid over the bcc. In these micellar systems, we anticipate similar behavior. Comparatively thin coronal layers have small local curvature corresponding to a convex coronal density profile. In this case the interactions between micelles are steeply repulsive. Micelles having longer coronal layers assume a profile better described by a concave function resulting in softer repulsions. We know the phase behavior is understood through a model of pair interactions between micelles; however, a quantitative description of the interactions is not yet available. While we are in the process of theoretically modeling the interactions between micelles in order to provide an accurate understanding of disorder-order transitions in micellar suspensions, currently we must rely on accessible experimental properties closely linked to the interactions to describe the phase behavior.

We classify these micelles by a ratio of the coronal layer thickness to the polystyrene core radius. The coronal layer thickness is obtained by subtracting the core radius from the hydrodynamic radius. The volume fraction of polystyrene corresponds to the volume fraction of the micellar core because the solvent swelling of the core is not appreciable. As a result, the phase diagram strongly resembles those for power-law [19] or Yukawa systems. As the length scale of the repulsion decreases, the disorder-order transition occurs at a higher concentration. In the limit of a very thin layer the micelles should behave like hard spheres, whose freezing transition from liquid to an fcc solid occurs at a volume fraction of 0.497 [1]. As the length scale of the repulsion increases, the disorder-order transition occurs at a lower core volume fraction and favors a bcc crystal. Strikingly, no bcc to fcc transition was observed in these systems. Upon increasing the concentration of a system known to undergo a liquid-bcc transition, we found a splitting of the first order Bragg peak and a loss of sphericity denoted by a shift in the location of the first minimum in the form factor. At these extreme concentrations, the strain on the micellar interface may give rise to shape transitions [20]. Shape transitions at very high polymer concentrations may account for some of the undetermined structures observed in the phase diagram. More detailed investigation is in progress to characterize block copolymer phase behavior in the presence of a selective solvent at very high polymer concentrations.

This work was supported by the NSF-MRL Program through the Stanford Center for Materials Research. The authors would like to thank Mark Fair and Min Lin for their assistance with these experiments.

[1] B. J. Alder, W. G. Hoover, and D. A. Young, J. Chem. Phys. **49**, 3688 (1968).
[2] J. Q. Broughton and G. H. Gilmer, J. Chem. Phys. **79**, 5095 (1983).
[3] P. N. Pusey and W. van Megen, Nature (London) **320**, 340–342 (1986).
[4] M. O. Robbins, K. Kremer, and G. S. Grest, J. Chem. Phys. **88**, 3286 (1988).
[5] Y. Monovoukas and A. P. Gast, J. Colloid Interface Sci. **128**, 533 (1989).
[6] S. D. Smith *et al.*, in *Polymer Solutions, Blends, and Interfaces*, edited by I. Noda and D. N. Rubingh (Elsevier, Amsterdam, 1992), pp. 43–64.
[7] K. A. Cogan, F. A. M. Leermakers, and A. P. Gast, Langmuir **8**, 429 (1992).
[8] A. Halperin, M. Tirrell, and T. P. Lodge, Adv. Polym. Sci. **100**, 31 (1992).
[9] K. A. Cogan, A. P. Gast, and M. Capel, Macromolecules **24**, 6512 (1991).
[10] M. Tirrell and N. Dan, Macromolecules **25**, 2890 (1992).
[11] M. Daoud and J. P. Cotton, J. Phys. (Paris) **43**, 531 (1982).
[12] S. T. Milner, T. A. Witten, and M. E. Cates, Macromolecules **21**, 2610 (1988).
[13] S. T. Milner, Science **251**, 905 (1991).
[14] S. T. Milner, Macromolecules **24**, 3074 (1991).
[15] T. P. Russell, in *Handbook of Synchrotron Radiation*, edited by G. Brown and D. E. Moncton (North-Holland, Amsterdam, 1991), Vol. 3.
[16] C. R. Harkless *et al.*, Phys. Rev. Lett. **64**, 2285 (1990).
[17] M. Shibayama, T. Hashimoto, and H. Kawai, Macromolecules **16**, 16 (1983).
[18] J. S. Higgins *et al.*, Polymer **27**, 931 (1986).
[19] W. G. Hoover, D. A. Young, and R. Grover, J. Chem. Phys. **56**, 2207 (1972).
[20] B. Gallot, Adv. Polym. Sci. **29**, 89 (1978).